

# Synthesis, Characterization, and Activity of Tin Oxide Nanoparticles: Influence of Solvothermal Time on Photocatalytic Degradation of Rhodamine B

Zuoli He<sup>1\*</sup>, Jiaqi Zhou<sup>2</sup>

<sup>1</sup>Electronic Materials Research Laboratory, School of Electronic and Information Engineering, Xi'an Jiaotong University, Xi'an, China

<sup>2</sup>School of Materials Science and Engineering, Shaanxi University of Science and Technology, Xi'an, China  
Email: \*wandaohzl@163.com, \*zlhe\_xjtu@163.com

Received April 26, 2013; revised June 9, 2013; accepted July 8, 2013

Copyright © 2013 Zuoli He, Jiaqi Zhou. This is an open access article distributed under the Creative Commons Attribution License, which permits unrestricted use, distribution, and reproduction in any medium, provided the original work is properly cited.

## ABSTRACT

The SnO<sub>2</sub> spheres-like nanoparticles have been successfully synthesized by a microwave solvothermal method, in which SnCl<sub>2</sub>·2H<sub>2</sub>O, poly(vinylpyrrolidone) PVP, H<sub>2</sub>O<sub>2</sub> and NaOH as raw materials. The as-synthesized products have been characterized by X-ray diffraction, scanning electron microscope, and UV/Vis/NIR spectrophotometer. Photocatalytic activities of the samples have been evaluated by the degradation of rhodamine B (RhB) under UV-light illumination. Results showed that these products with diameter about 1 - 2 μm, and when the reaction time prolong, the surface of the SnO<sub>2</sub> spheres will change to rough and then smooth when the time even longer. The product with nanorods on its surface shows the higher photocatalytic activity and red shift in the UV-vis absorption, which are relative to the unique structure. At last we studied the electron transfer reactions during photo-oxidation of RhB.

**Keywords:** SnO<sub>2</sub>; Nanoparticles; Photocatalytic; Solvothermal

## 1. Introduction

Environmental problems, especially, the sustained pollutions of water by various organic and metallic ion contaminants have been one of the most serious problems. And many efforts are dedicated to the remediation of environmental pollution [1-3]. For instance, photodegradation of organic compounds provides an available way to deal with the water pollution. Nanostructured semiconductors (such as TiO<sub>2</sub>, ZnO, SnO<sub>2</sub> and so on) are proved to be an excellent photocatalyst which can degrade many kinds of persistent organic pollution [4-10].

Tin oxide (SnO<sub>2</sub>), as one of the most important semiconductor oxides, has been used as photocatalyst for photodegradation of organic compounds. The results indicate that SnO<sub>2</sub> has exhibited photoactivity toward degradation of dye and other organic compounds [11,12]. However, just like other transition metal oxides photocatalysts such as TiO<sub>2</sub> and ZnO, SnO<sub>2</sub> suffer from low photocatalytic efficiency because of its wide-bandgap (energy of the band gap is about 3.6 eV) [13] and high recombination rates of photogenerated electron-hole pairs. This defects

hinder SnO<sub>2</sub> photocatalyst using widely and practically in the environmental application [14]. To overcome this problem, the fabrication of nanostructures provides an effective way.

The synthesis of TiO<sub>2</sub>-based photocatalysts has been reported in our previous papers [15-18]. Recently, SnO<sub>2</sub>-based photocatalysts were also synthesized by various approaches and have exhibited attractive performances [19-22]. In this work, we describe the synthesis of SnO<sub>2</sub> nanoparticles via a microwave solvothermal method and discuss the effect of solvothermal time on the morphologies and nanostructures. The as-synthesized SnO<sub>2</sub> nanoparticles were well characterised and their photocatalytic activities were evaluated by the photodegradation of Rhodamine B (RhB).

## 2. Experimental

### 2.1. Preparation

All the reagents used in this experiment were analytical grade and were used without further purification. In a typical preparation procedure, first, 1.353 g of SnCl<sub>2</sub>·2H<sub>2</sub>O was dissolved into 40 mL distilled water under conti-

\*Corresponding author.

nuous magnetic stirring to form white slurry. Then 1.44 g of NaOH and 5 mL of 30% H<sub>2</sub>O<sub>2</sub> were introduced to the well-stirred mixture at room temperature with simultaneous vigorous agitation until NaOH dissolved completely. When the solution became transparent, 1.2 g of poly (vinylpyrrolidone) PVP (MW 30,000) was introduced. After several minutes of stirring, Subsequently, the obtained solution was transferred into five 100 mL teflon autoclaves, which was treated in a MDS-8 microwave hydrothermal system (manufactured by Shanghai Sineo Microwave Chemistry Technology Co. Ltd.) at 180°C for 30 min, 60 min, 90 min, respectively, and allowed to cool to room temperature naturally. The resulting white powder was collected from the bottom of the Teflon container after decanting the supernatant, washed several times with absolute ethanol and distilled water. Subsequently, the products were dried in vacuum at 60°C for 12 h for further characterization.

## 2.2. Characterization

Morphologies of the samples were observed by using a high-resolution field emission scanning electron microscope (JSM-6700). All the images were obtained under high vacuum mode without sputter coating. X-Ray Diffraction (D/max-2200, Diffractometer with Cu K $\alpha$  radiation) was used to verify crystal phase and estimate the crystal sizes of as-synthesized SnO<sub>2</sub> nanoparticles. Absorption spectrum was measured on a UV/Vis/NIR spectrophotometer (LAMBDA-950) in the wavelength range of 200 - 800 nm.

## 2.3. Photocatalytic Activity Measurement

The photocatalytic activity of as-synthesized SnO<sub>2</sub> nanoparticles was evaluated through the degradation of 5 mg/L Rhodamine B (RhB) in a BL-GHX-V multifunctional photochemical reactor (Shanghai Bilon Experiment Equipment Co. Ltd., Shanghai, China). The volume of the reaction solution was 250 mL (8 test tubes of 30 mL) into which 25 mg of photocatalyst was added and stirred for 30 min. The solution was dispersed by sonication, and then transferred to test tubes. Irradiation was provided by a medium-pressure Hg lamp (300 W), and the reaction temperature was kept about 25°C. Stirring was performed at all the times during the reaction. Sampling was also performed at regular intervals (every 15 min). The residual concentration of RhB was determined by measuring its absorbance at 554 nm using an UV/Vis/NIR spectrophotometer (LAMBDA-950).

## 3. Results and Discussion

### 3.1. SEM and XRD Analysis

XRD pattern of the as-prepared product is shown in **Figure 1**. All the diffraction peaks are quite similar to those

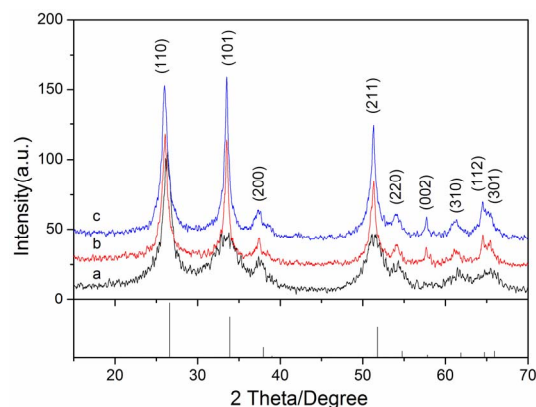


**Figure 1.** XRD patterns of the SnO<sub>2</sub> nanoparticles synthesized with different reaction time: (a) 30 min; (b) 60 min; (c) 90 min.

of SnO<sub>2</sub>, which can be indexed as the tetragonal rutile structure of SnO<sub>2</sub> with lattice constants of  $a = 4.738 \text{ \AA}$  and  $c = 3.187 \text{ \AA}$ , which is in good agreement with the JCPDS file of SnO<sub>2</sub> (JCPDS 41 - 1445) [22]. No impurity diffraction peaks are observed, indicating the high purity of the final products. In additionally, when treated for 30 min, the diffraction peaks were broaden and weaken, due to the relative lower crystallinity and size-quantization effect of nanomaterials (shown in **Figure 1(a)**). The increase of crystallinity was corresponding to the reaction times during the solvothermal process, it clearly show when reacted 90 min, the sample has the most high crystallinity among these samples. According to the Scherrer equation,  $D = K\lambda/(\beta \cos \theta)$ , the average crystallite sizes of SnO<sub>2</sub> calculated from the main diffraction peak are about 9, 16 and 17 nm, respectively.

Scanning electron microscopy (SEM) image of the as-grown product were shown in **Figure 2**, the nanoparticles were seem to spheres, and the diameters about 1 - 2  $\mu\text{m}$  are clearly observed. Higher magnification SEM image shown in **Figure 2(b)** demonstrate the detailed structural information of the sample prepared during 30 min heat treatment. As can be seen in **Figure 2(b)**, the observed SnO<sub>2</sub> spheres are seem to be soft and have some holes, due to the effect of PVP. So we can indicate that the process of formation of the sphere is not completed and this is just a middle product. When the time prolong to 60 min, the spheres made up of numerous one-dimensional tetragonal prism nanorods with an average diameter of about 100 nm were clearly seen in **Figure 2(d)**. Interestingly, when continue prolong the time to 90 min, the surface become smooth, but the nanorods also can be seen (shown in **Figure 2(f)**). I think the nano-sized particles (as shown in **Figure 2(d)**) around the sphere will gather on the surface of the sphere, and close the hole between nanorods. This process was simply shown in **Figure 3**, the nanoparticles will show this process in the solvothermal process, and when this will con-

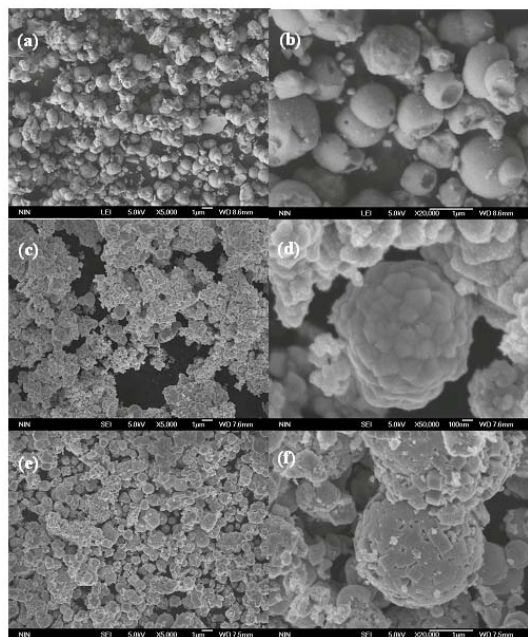


**Figure 2.** FESEM images of the SnO<sub>2</sub> nanoparticles synthesized by microwave solvothermal method with different reaction time: (a) (b) 30 min, (c) (d) 60 min, (e) (f) 90 min.

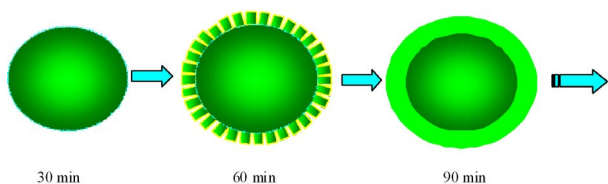


**Figure 3.** Schematic diagram of the microwave solvothermal process with time increase.

tinue occur when the time even longer. And this will also lead to the size of nanocrystals and diameter of the sphere increase. The BET surface areas of the sample were obtained from N<sub>2</sub> adsorption/desorption isotherms determined at liquid nitrogen temperature on an automatic analyzer (Micromeritics, ASAP 2010), and the BET surface area of the samples are 45.1, 56.5, 50.9 m<sup>2</sup>/g, respectively.

### 3.2. UV-Vis Analysis

**Figure 4** shows the absorption spectra of the samples, which are all nearly identical, indicating that their optical band gaps were also almost the same. The fundamental absorption edge of SnO<sub>2</sub> located in the UV region at about 325 nm. But they also show some differences, as shown in **Figure 4** inset curves. The fundamental absorption edges were 327.5, 328.5 and 352.0 respectively. The products prepared during 60 min were shown a little red shift due to the unique nanostructures and creation of oxygen vacancies [15]. It will narrow the band gap and enhance the UV absorption.

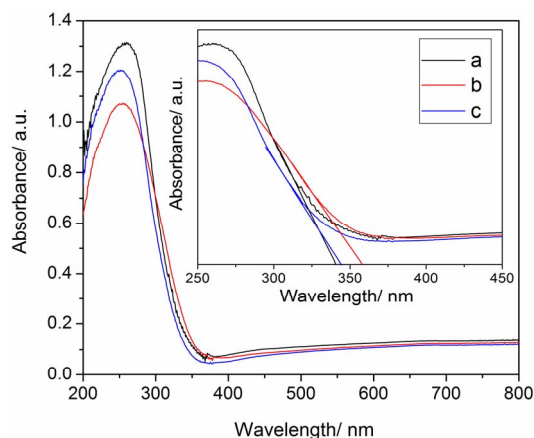


**Figure 4.** UV-visible absorption spectra of the SnO<sub>2</sub> nanoparticles synthesized by microwave solvothermal method with different reaction time: (a) 30 min; (b) 60 min; (c) 90 min. Inset was show the absorption at the range of 250 - 450 nm.

### 3.3. Evaluation of Photocatalytic Activities

Photocatalytic activity of the synthesized SnO<sub>2</sub> products was evaluated by monitoring the change in optical absorption of an RhB solution at ~554 nm during its photocatalytic decomposition process. The kinetics of this reaction can be monitored by UV-vis spectroscopy as seen from UV-vis spectra measured at different times shown in **Figures 5(a)-(c)**. It demonstrates RhB shows a strong absorption band at 554 nm and the addition of SnO<sub>2</sub> products leads to a decrease of the absorption band with time. The color of the dispersion disappeared, indicating that the chromophoric structure of the dye was destroyed. The order rate kinetics with respect to the RhB concentration could be used to evaluate the photocatalytic rate as done previously. As it clearly demonstrated the SnO<sub>2</sub> photocatalysts show higher photocatalytic activity. **Figure 5(d)** shows a comparison of the photocatalytic activities among SnO<sub>2</sub> photocatalyst treated in different times. Additional experiments in the absence of photocatalyst, was also present in **Figure 5(d)**. It can be noted that a trend of the photocatalytic activity is as follow order: b > a > c. The photocatalytic can be attributed to UV absorption, and the products prepared during 60 min shows a red shift and shows the higher photocatalytic activity. The existing of the nanorods also increases the surface area and there is more reaction place during photocatalytic process [18].

At last, we study the mechanism for photocatalytic degradation of RhB, and the electron transfer reactions involved in the selective photooxidation of RhB with oxygen are proposed in **Figure 6**. When the SnO<sub>2</sub> photocatalyst is excited under light irradiation with greater energy than its band gap energy, it will cause the formation of the hole-electron pair in the SnO<sub>2</sub>, Subsequently,

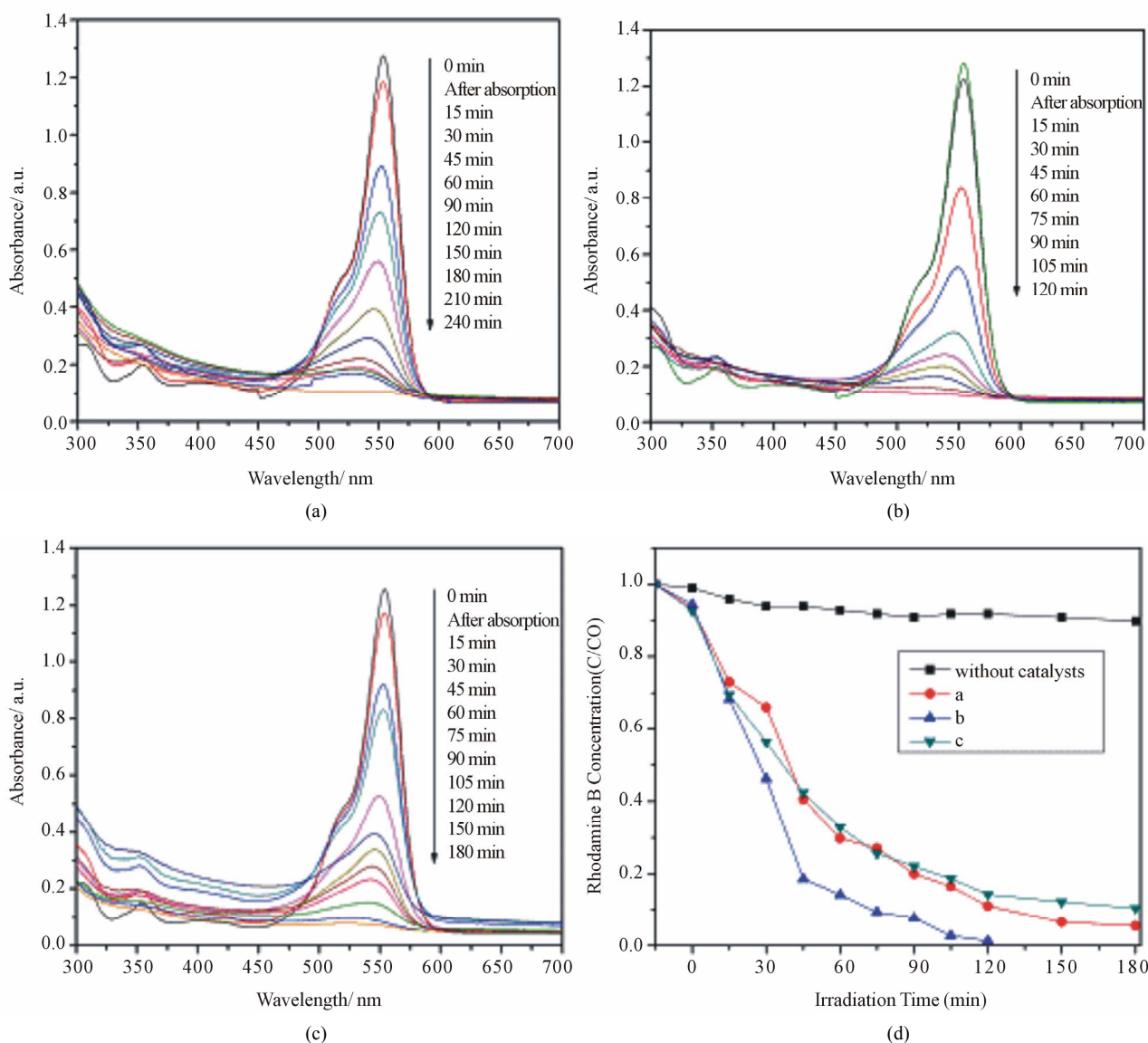


**Figure 5. Photocatalytic degradation of RhB solutions under UV irradiation by the presence of SnO<sub>2</sub> nanoparticles synthesized in different time: (a) 30 min, (b) 60 min, (c) 90 min. The concentration of the reactants was as follow: [RhB] = 5 mg/L, [SnO<sub>2</sub>] = 100 mg/L.**

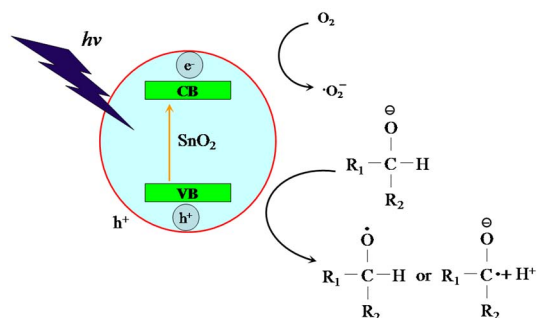


**Figure 6. Electron transfer reactions with RhB.**

redox reactions can occur superoxide ions and hydroxyl radicals which are nonselective strong oxidizing agents,

Hole ( $h^+$ ) with high activity may react with H<sub>2</sub>O or hydroxyl groups adsorbed on the surface of the SnO<sub>2</sub>, the formed hydroxyl radicals also have strong oxidizing activity Hole ( $h^+$ ) and Electron ( $e^-$ ) can react with the dye molecule in favor of its degradation directly and following mineralization. In the process, the RhB can interact with the photogenerated holes in the valence band (VB), and provides a direct chemical reaction between the dye and the photocatalyst [23].

#### 4. Conclusion

In summary, we studied the SnO<sub>2</sub> photocatalyst prepared via microwave solvothermal process. When the reaction time prolong, the surface of the SnO<sub>2</sub> spheres

will change to rough and then smooth when the time even longer. We also propose the modeling to explain this interesting phenomenon. The product with nanorods on its surface shows the higher photocatalytic activity and red shift in the UV-vis absorption, which are relative to the unique structure.

## 5. Acknowledgements

This work was supported by the Research Fund for the Doctoral Program of Higher Education of China under grant 20120201130004, the Science and Technology Developing Project of Shaanxi Province (2012KW-11), and the Fundamental Research Funds for the Central Universities.

## REFERENCES

- [1] C. Burda, X. Chen, R. Narayanan and M. A. El-Sayed, "Chemistry and Properties of Nanocrystals of Different Shapes," *Chemical Reviews*, Vol. 105, No. 4, 2005, pp. 1025-1102. [doi:10.1021/cr030063a](https://doi.org/10.1021/cr030063a)
- [2] X. Chen and S. S. Mao, "Titanium Dioxide Nanomaterials: Synthesis, Properties, Modifications, and Applications," *Chemical Reviews*, Vol. 107, No. 7, 2007, pp. 2891-2959. [doi:10.1021/cr0500535](https://doi.org/10.1021/cr0500535)
- [3] Z. He, W. Que, J. Chen, X. Yin, Y. He, J. Ren, "Photocatalytic Degradation of Methyl Orange over Nitrogen-Fluorine Codoped TiO<sub>2</sub> Nanobelts Prepared by Solvothermal Synthesis," *ACS Applied Materials & Interfaces*, Vol. 4, No. 12, 2012, pp. 6816-6826. [doi:10.1021/am3019965](https://doi.org/10.1021/am3019965)
- [4] J. C. Yu, J. G. Yu, W. K. Ho, Z. T. Jiang and L. Z. Zhang, "Effects of F Doping on the Photocatalytic Activity and Microstructures of Nanocrystalline TiO<sub>2</sub> Powders," *Chemistry of Materials*, Vol. 14, No. 9, 2002, pp. 3808-3816. [doi:10.1021/cm020027c](https://doi.org/10.1021/cm020027c)
- [5] J. Ng, J. H. Pan and D. D. Sun, "Hierarchical Assembly of Anatase Nanowhiskers and Evaluation of Their Photocatalytic Efficiency in Comparison to Various One-Dimensional TiO<sub>2</sub> Nanostructures," *Journal of Materials Chemistry*, Vol. 21, No. 32, 2011, pp. 11844-11853. [doi:10.1039/c1jm11088h](https://doi.org/10.1039/c1jm11088h)
- [6] Z. He, W. Que, Y. He, J. Chen, H. Xie and G. Wang, "Nanosphere Assembled Mesoporous Titanium Dioxide with Advanced Photocatalytic Activity Using Absorbent Cotton as Template," *Journal of Materials Science*, Vol. 47, No. 20, 2012, pp. 7210-7216. [doi:10.1007/s10853-012-6667-9](https://doi.org/10.1007/s10853-012-6667-9)
- [7] C. A. Martinez-Huitle and E. Brillas, "Decontamination of Wastewaters Containing Synthetic Organic Dyes by Electrochemical Methods: A General Review," *Applied Catalysis B: Environmental*, Vol. 87, No. 4-5, 2009, pp. 105-145. [doi:10.1016/j.apcatb.2008.09.017](https://doi.org/10.1016/j.apcatb.2008.09.017)
- [8] H. J. Zhang, G. H. Chen and D. W. Bahnemann, "Photoelectrocatalytic Materials for Environmental Applications," *Journal of Materials Chemistry*, Vol. 19, No. 29, 2009, pp. 5089-5121. [doi:10.1039/b821991e](https://doi.org/10.1039/b821991e)
- [9] H. J. Wang, F. Q. Sun, Y. Zhang, K. Y. Gu, W. Chen and W. S. Li, "Photochemical Construction of Free-Standing Sn-Filled SnO<sub>2</sub> Nanotube Array on a Solution Surface for Flexible Use in Photocatalysis," *Journal of Materials Chemistry*, Vol. 21, No. 33, 2011, pp. 12407-12413. [doi:10.1039/c1jm10887e](https://doi.org/10.1039/c1jm10887e)
- [10] Z. He and W. Que, "Enhanced Photocatalytic Activity of N-Cetyl-N,N,N-Trimethyl Ammonium Bromide-Assisted Solvothermal Grown Fluff-Like ZnO Nanoparticles," *Journal of Nanoengineering and Nanomanufacturing*, Vol. 2, No. 1, 2012, pp. 17-21. [doi:10.1166/jnan.2012.1043](https://doi.org/10.1166/jnan.2012.1043)
- [11] M. Dimitrov, T. Tsoncheva, S. Shao and R. Köhn, "Novel Preparation of Nanosized Mesoporous SnO<sub>2</sub> Powders: Physicochemical and Catalytic Properties," *Applied Catalysis B: Environmental*, Vol. 94, No. 1-2, 2010, pp. 158-165. [doi:10.1016/j.apcatb.2009.11.004](https://doi.org/10.1016/j.apcatb.2009.11.004)
- [12] S. S. Wu, H. Q. Cao, S. F. Yin, X. W. Liu and X. R. Zhang, "Amino Acid-Assisted Hydrothermal Synthesis and Photocatalysis of SnO<sub>2</sub> Nanocrystals," *The Journal of Physical Chemistry C*, Vol. 113, No. 41, 2009, pp. 17893-17898. [doi:10.1021/jp9068762](https://doi.org/10.1021/jp9068762)
- [13] Y. T. Han, X. Wu, Y. L. Ma, L. H. Gong, F. Y. Qu and H. J. Fan, "Porous SnO<sub>2</sub> Nanowire Bundles for Photocatalyst and Li Ion Battery Applications," *CrystEngComm*, Vol. 13, No. 10, 2011, pp. 3506-3510. [doi:10.1039/c1ce05171g](https://doi.org/10.1039/c1ce05171g)
- [14] Z. Wen, G. Wang, W. Lu, Q. Wang, Q. Zhang and J. Li, "Enhanced Photocatalytic Properties of Mesoporous SnO<sub>2</sub> Induced by Low Concentration ZnO Doping," *Crystal Growth & Design*, Vol. 7, No. 9, 2007, pp. 1722-1725. [doi:10.1021/cg060801z](https://doi.org/10.1021/cg060801z)
- [15] Z. He, W. Que, H. Xie, J. Chen, Y. Yuan and P. Sun, "Facile Synthesis of Self-Sensitized TiO<sub>2</sub> Photocatalysts and Their Higher Photocatalytic Activity," *Journal of The American Ceramic Society*, Vol. 95, No. 12, 2012, pp. 3941-3946. [doi:10.1111/j.1551-2916.2012.05426.x](https://doi.org/10.1111/j.1551-2916.2012.05426.x)
- [16] Z. He, W. Que, Y. He, J. Chen, J. Hu, H. Javed, Y. Ji, X. Li and D. Fei, "Electrochemical Behavior and Photocatalytic Performance of Nitrogen-Doped TiO<sub>2</sub> Nanotubes Arrays Powders Prepared by Combining Anodization with Solvothermal Process," *Ceramics International*, Vol. 39, No. 5, 2013, pp. 5545-5552. [doi:10.1016/j.ceramint.2012.12.068](https://doi.org/10.1016/j.ceramint.2012.12.068)
- [17] Z. He, W. Que, J. Chen, Y. He and G. Wang, "Surface Chemical Analysis on the Carbon-Doped Mesoporous TiO<sub>2</sub> Nanoparticles after Post-thermal Treatment: XPS and FTIR Characterization," *Journal of Physics and Chemistry of Solids*, Vol. 74, No. 7, 2013, pp. 924-928. [doi:10.1016/j.jpcs.2013.02.001](https://doi.org/10.1016/j.jpcs.2013.02.001)
- [18] Z. He, Z. Zhu, J. Li, N. Wei and J. Zhou, "Characterization and Activity of Mesoporous Titanium Dioxide beads with High Surface Areas and Controllable Pore Sizes," *Journal of Hazardous Materials*, Vol. 190, No. 1-3, 2011, pp. 133-139. [doi:10.1016/j.jhazmat.2011.03.011](https://doi.org/10.1016/j.jhazmat.2011.03.011)
- [19] E. M. Seftel, E. Popovici, M. Mertens, E. A. Stefaniak, R. V. Grieken, P. Cool and E. F. Vansant, "SnIV-Containing Layered Double Hydroxides as Precursors for Nano-Sized ZnO/SnO<sub>2</sub> Photocatalysts," *Applied Catalysis B: Environmental*, Vol. 84, No. 3-4, 2008, pp. 699-705. [doi:10.1016/j.apcatb.2008.06.006](https://doi.org/10.1016/j.apcatb.2008.06.006)

- [20] C. Wang, J. C. Zhao, X. M. Wang, B. X. Mai, G. Y. Sheng, P. A. Peng and J. M. Fu, "Preparation, Characterization and Photocatalytic Activity of Nano-Sized ZnO/SnO<sub>2</sub> Coupled Photocatalysts," *Applied Catalysis B: Environmental*, Vol. 39, No. 3, 2002, pp. 269-279. [doi:10.1016/S0926-3373\(02\)00115-7](https://doi.org/10.1016/S0926-3373(02)00115-7)
- [21] N. Wang, J. X. Xu and L. H. Guan, "Synthesis and Enhanced Photocatalytic Activity of Tin Oxide Nanoparticles Coated on Multi-Walled Carbon Nanotube," *Materials Research Bulletin*, Vol. 46, No. 9, 2011, pp. 1372-1376. [doi:10.1016/j.materresbull.2011.05.014](https://doi.org/10.1016/j.materresbull.2011.05.014)
- [22] L. R. Zheng, Y. H. Zheng, C. Q. Chen, Y. Y. Zhan, X. Y. Lin, Q. Zheng, K. M. Wei and J. F. Zhu, "Network Structured SnO<sub>2</sub>/ZnO Heterojunction Nanocatalyst with High Photocatalytic Activity," *Inorganic Chemistry*, Vol. 48, No. 5, 2009, pp. 1819-1825. [doi:10.1021/ic802293p](https://doi.org/10.1021/ic802293p)
- [23] Z. Zhu, J. Zhou and Z. He, "Effects of Heat Treatment Scheme on Luminescence Properties and Photocatalytic Activity of Mo<sub>2</sub>O<sub>3</sub>/TiO<sub>2</sub> Nanowire Prepared via Solvothermal Method," *Journal of Nanoengineering and Nanomanufacturing*, Vol. 2, No. 1, 2012, pp. 80-84. [doi:10.1166/jnan.2012.1055](https://doi.org/10.1166/jnan.2012.1055)